Article

Experimental Investigation on Bituminite Dust Suppression Characteristics of a Bonding-Wetting Composite Dust Suppressant

Chunshan Zheng,* Suqian Qian, Bingyou Jiang, Sheng Xue, Xiaohan Wang, Cancan Li, and Mingyun Tang

Read Online

ACCESS | Metrics & More | Article Recommendations

ABSTRACT: In order to reduce the occupational health hazard of coal dust to miners, surface tension and viscosity tests and bituminous coal powder sedimentation experiments were conducted. A composite dust suppressant with bonding-wetting effects was developed. Meanwhile, based on the FTIR test and peak-differentiating curve fitting, the changes of peak areas of coal samples before and after dust suppressant treatment were investigated, with quantitative analysis on hydrophilic and hydrophobic groups. Gravity drop weight tests and Malvern particle size analyses were carried out. The particle size distribution was studied based on the Boltzmann function model. The characteristic particle size theory was adopted to analyze dust reduction performance and time's effect on the performance. Results show that the surface tension of the composite dust suppressant is 31.02 ± 0.09 mN/m with the viscosity being 84.60 mPa·s for the mixture of 0.1% SDS solution and 0.4% CMC-Na solution being 1:5. The ratio of the hydrophilic group of bituminous coal reaches 97.37% affected by the dust suppressant with a good wetting and cohesiveness effect. The characteristic particle size D_{10} of dust increases by 11.77 and 46.67%, D_{50} rises by 7.56 and 36.89%, and D_{90} grows by 10.56 and 32.96%, respectively. The compressive strengths of the Shenmu coal sample and Lucun coal sample increase by 82.86 and 66.72% compared with that of raw coal after 48 h of dust suppressant treatment. The breakage degree at the end face of treated coal is smaller than that of raw coal. The composite dust suppressant makes the particles in coal more cohesive and effectively weakens the dust-producing property. Research results are of practical significance for improving the effect of water injection on dust reduction.
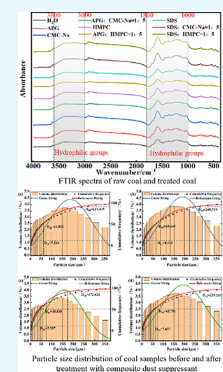
1. INTRODUCTION

Dust is one of the major occupational health hazards threatening miners. Coal seam hydraulic injection is widely adopted in dust reduction practice.[1] However, some coal seams with a high gas content and low permeability face challenges in water injection. The conventional low-pressure hydraulic injection methods often struggle to effectively wet the coal, significantly reducing the dust reduction efficacy. Meanwhile, merely increasing injection pressure to enhance effectiveness may lead to localized stress concentration in coal seams, rising the risk of coal and gas outburst.[2,3] Therefore, improvements in water injection processes and the addition of water injection solvents are necessary to enhance the dust control efficacy of water injection.

Related scholars have conducted a large amount of research on coal seam water injection processes and wetting agents. Ya et al. analyzed the change characteristics of coal parameters after injecting pure water and a wetting agent. They found that the wetting agent could well reduce the contact angle of coal.[4] Xiaotao used a gas extraction borehole to carry out the coal seam water injection experiment. The injection of aqueous solution with an active agent greatly improved the dust reduction efficiency.[5] Yansong proposed that the addition of surfactants can reduce the surface tension of water, reduce the

interface contact angle between water and coal, increase the capillary force of aqueous solution in small pores, and finally improve the content of water in coal.[6] Chao has done related experimental studies on the wetting performance of surfactants. It was obtained that the wetting performance of most surfactants after compounding gets better. However, the effects are different, with the wetting effect of a certain compounding surfactant decreasing.[7,8] Wang et al. studied the influence of the ratio of different surfactants on water injection effects. By comparing the contact angle, the best compound ratio was determined.[9] In order to improve the on-site application effect of coal seam water injection, Haifei et al. measured impacts of four noncationic surfactants of SDBS, SDS, AEO, and TX-100 on wetting characteristics of coal. The wetting performance of SDBS and SDS on coal was better than that of AEO and TX-100.[10] Zongqi et al. selected five nonionic and anionic surfactants for compound experimental research,

developing an efficient dust inhibitor for bituminous coal. The best compound volume ratio is 7:3, which is more conducive to the improvement of dust reduction efficiency.[11] Chao et al. adopted surfactants to combine with inorganic salts to develop a new compound wetting agent.[12] Zhang et al. analyzed the surface tension and functional group test results of 10 different anions and cations to reveal enhanced wettability of coal dust by surface-active ionic liquids.[13] Xie et al. developed a wetting agent formula based on characteristics of the surface tension and contact angle. Through nuclear magnetic resonance testing, it was determined that the compound acid-containing reagent (HCl+HF+SDS+NaCl) had good coal wetting properties.[14] Xu et al. revealed the influence of oxygen-containing functional groups and minerals on coal wettability and explained the micromechanism of SDBS and SDS wetting the coal.[15] Liu et al. found that the content of cyclohydroxyl and OH:O has the most significant relationship with the contact angle. This research result is of practical significance for improving the effect of water injection and dust reduction on coal seams.[16]

In recent years, research on water injection dust suppressants has focused on the selection and compounding of wetting surfactants. While wetting surfactants show dust suppression effects, some agents have environmental implications and exhibit short-lived wetting effects on coal. To address these issues, especially for enhancing dust suppression effects on loose coal formations, the development of composite dust suppressants with both wetting and cohesive properties is essential. This study evaluates the wetting performance of experimental bituminous coal based on sedimentation time and surface tension. The types and concentrations of binders and wetting agents are determined, which are used to compound the bonding-wetting composite dust suppressant. Meanwhile, changes in coal composition, mechanical strength, and dust physicochemical properties are investigated before and after treatment with composite dust suppressants. The mechanisms of dust suppression by composite agents are revealed through analysis of variations of hydrophilic functional group peak areas, coal compressive strength, and coal dust particle size distribution, providing valuable insights for enhancing water injection agents and injection processes to improve dust reduction efficiency.

2. DUST SUPPRESSANT COMPOUNDING AND ITS PERFORMANCE ANALYSIS

The coal samples used in this experiment were Lucun bituminous coal and Shenmu bituminous coal. As the chemical composition of coal samples has an important impact on the wetting characteristics, the industrial composition and element analyses of coal samples were carried out. As shown in Table 1, the content of nonhydrophilic components such as carbon organic matter of those two bituminous coals is at a high level. The fixed carbon contents are 66.33 and 54.23%, while the ash contents are only 3.49 and 11.87%. The hydrophilic component content is at a low level. Thus, the coal sample had strong hydrophobicity. Therefore, it is necessary to

improve the wetting effect of coal by adding water injection reagents.

2.1. Analysis of Binder Monomers. The binders sodium carboxymethyl cellulose (CMC-Na) and hydroxypropyl methyl cellulose (HMPC) are both green reagents. CMC-Na is an ether starch, which is a modified starch. It is nontoxic, tasteless, and soluble in water and has a wide range of sources and low price. HMPC is a propylene glycol ether of methyl cellulose, which is a white powder and soluble in cold water, and has the characteristics of pH stability, water retention, and excellent film forming.[17] According to eq 1, binders of different concentrations were prepared separately: CMC-Na solution and HMPC solution with mass fractions of 0.15, 0.2, 0.3, 0.4, 0.5, 0.6, and 0.7% for experimental testing.

$$C_1V_1 = C_2V_2 \tag{1}$$

where C_1 is the initial solution concentration (mol/L), V_1 is the initial solution volume (L), C_2 is the concentration of the prepared solution (mol/L), and V_2 is the volume of the prepared solution (L).
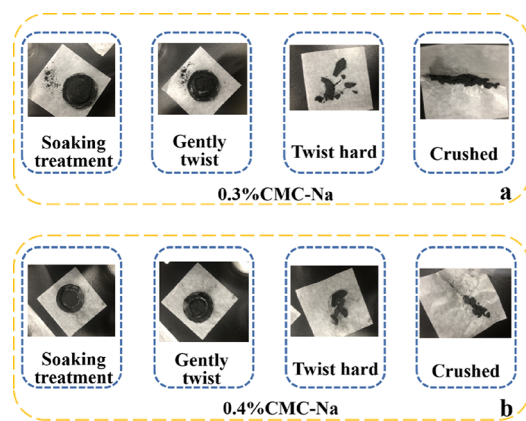
Multiple 0.2 g samples of Shenmu bituminous coal dusts of 200 mesh were weighed and then placed at the bottom of the cup. A rubber-tipped buret was used to inhale the CMC-Na solution, HMPC solution, and the appropriate amount of water, dripping to the coal dust. With the solution dripping, liquid beadlike small clusters were formed in the upper layer of coal dust, as shown in Figure 1.
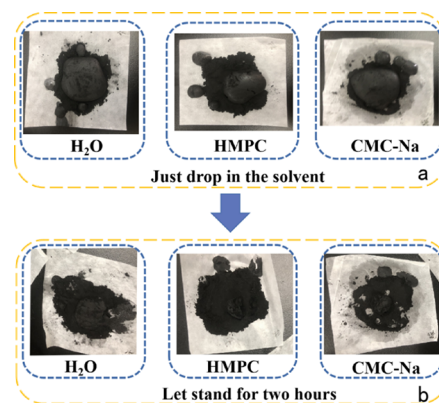
Figure 1. (a,b) Changes of the agglomeration degree of pulverized coal affected by different binders and water.

Due to the surface tension of water being approximately 72 mN/m, the surface tension of prepared CMC-Na solutions ranges from 72.49 ± 0.05 to 72.58 ± 0.1 mN/m, and HMPC solutions range from 72.28 ± 0.06 to 72.49 ± 0.08 mN/m. High surface tension affects wetting. After 2 h of standing, there are obvious thin films. However, the droplets formed by dripping water onto the coal powder's surface are easily broken, leading to the solution leaking out and the film deflating. The droplets formed by treating the coal powder with CMC-Na and HMPC solutions do not break, forming a shell-like structure after 1 week. When being lightly touched, there is no obvious change, but localized breakage occurs when being pinched lightly, and overall breakage requires forceful pinching, indicating strong adhesion as shown in Figure 2.

The binder formed a network structure inside the coal, providing a good skeleton effect and resulting in a shell-like structure. Additionally, as shown in Figure 2, with an increase in the amount of the binder, more solid structures are formed,

Table 1. Results of Industrial Analysis of Coal Samples

| coal type	Mad%	Aad%	Vad%	Fcad%
Lucun bituminous coal	2.40	3.49	27.78	66.33
Shenmu bituminous coal	6.92	11.87	26.98	54.23

Figure 2. (a,b) Effect of CMC-Na solution with different mass fractions on coal powder bonding.

providing a better support inside the coal powder, resulting in improved adhesion.[18,19] Furthermore, adhesion does not change significantly over time, indicating good stability.

The bonding and aggregation capabilities of coal powder particles could be represented by viscosity, which is an important indicator of the dust suppressant performance. The viscosities of the two binders were measured using an NDJ-8S digital rotational viscometer. The prepared solutions were poured into containers. A suitable rotor was selected and connected to the screw of the viscometer, and the rotor was placed on the upper end of the center of the solution. The pulley was adjusted so that the solution to be measured was completely submerged in the measurement mark, and the viscometer was adjusted to start the measurement of the viscosity of solution until the data were stable. If the percentage of the display reading was less than 10, then it meant that the rotor selection was not appropriate; it should be replaced with a larger-diameter rotor, and the range should be reset, trying to make the percentage close to 50%. The viscosity of each concentration of binder solution was measured three times to obtain average results, shown in Figure 3.[20]

As can be seen in Figure 3, there are some differences in the viscosity of the two binders, both of which increase with the rising mass fraction. Among them, the viscosity of CMC-Na solution increases faster with its mass fraction and grows faster between 0.15 and 0.7%. The viscosity values of 0.15% CMC-Na solution and 0.15% HMPC solution do not differ much and
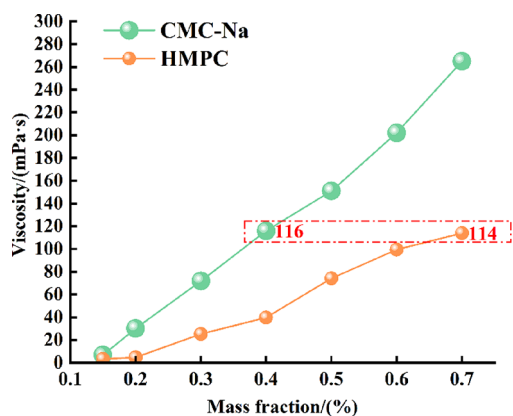
Figure 3. Results of the viscosity measurement of two binders.

are lower than 20 mPa·s. While the viscosity of HMPC solution is lower than 0.2%. Its viscosity value and change are both small. When the mass fraction of two solutions reaches 0.3%, it could meet the viscosity demand of the dust suppressant. When the mass fraction of HMPC solution is 0.7%, the viscosity is 114 mPa·s. With the mass fraction being over 0.7%, the solution tends to be in a viscous paste state. In this case, the large viscosity could cause blockage of fissures in coal and affect the injection effect of the dust suppressant. The HMPC solution with a mass fraction of 0.7% is selected for the subsequent test. At the same mass fraction, the viscosity of CMC-Na solution is higher than that of HMPC solution. When the mass fraction of CMC-Na solution reaches 0.6%, the viscosity is more than 200 mPa·s. The larger viscosity affects the effect of dust reduction. Hence, the CMC-Na solution with a mass fraction of 0.4−0.6% could be selected for the subsequent test. Meanwhile, when the mass fraction of CMC-Na solution reaches 0.4%, the viscosity is 116 mPa·s, which is similar to the viscosity of HMPC solution with a mass fraction of 0.7%. Therefore, the CMC-Na solution with a mass fraction of 0.4% is selected for the subsequent test.

2.2. Surfactant Addition Design. In order to solve the problem of poor wettability of pure binders, surfactants that could reduce surface tension are added. Surfactants have hydrophilic properties and are usually used as water injection additives in the water injection process, which significantly increases the water injection wetting effect. To meet requirements of nontoxic, noncorrosive, environmentally friendly, widely available, and low-cost performance, surfactants suitable for the characteristics of experimental coal quality are selected: anionic surfactant sodium dodecyl sulfate (SDS) and nonionic surfactant alkyl polyglycoside (APG).[21] SDS is a generally white or light-yellow powder and soluble in water, with good emulsification, penetration, decontamination, and dispersion. APG is a generally colorless to light-yellow liquid with low surface tension, good wettability, and compatibility. The surface tension values of those surfactants at different concentrations are measured to decide the most effective surfactants and the optimal proportioning concentration.

Anionic surfactant SDS and nonionic surfactant APG solutions with concentrations of 0.05, 0.1, 0.15, 0.2, 0.25, and 0.3% were prepared. The surface tensions of the above solutions with different concentrations were measured. It is found that the APG solution with a mass fraction of 0.15% and the SDS solution with a mass fraction of 0.1% have lower surface tensions of 27.93 ± 0.02 and 28.26 ± 0.09 mN/m, respectively. The 0.1% SDS solution and 0.15% APG solution were compounded with the 0.4% CMC-Na solution and 0.7% HMPC solution, respectively. The volume ratios of compounding solutions are 1:9, 1:8, 1:7, 1:6, 1:5, 1:4, 1:3, 1:2, 1:1, and 1:0. The surface tension, settling speed of coal powder, and viscosity of composite dust suppressant solutions with different volume ratios were tested and analyzed to determine the optimal ratio.[22]

2.3. Analysis of Composite Dust Suppressant Characteristics. *2.3.1. Surface Tension.* Common methods for surface tension measurement include the capillary rising method, platinum plate method, ring method, bubble pressure method, and drop weight method.[23] In this experiment, the platinum plate method was adopted to measure the surface tension of 10 different composite solutions at varying ratios, with results shown in Table 2.

Table 2. Surface Tension of Different Dust Suppressants

compound ratio	SDS+CMC-Na surface tension (mN/m)	SDS+HMPC surface tension (mN/m)	APG+CMC-Na surface tension (mN/m)	APG+HMPC surface tension (mN/m)
1:9	39.12 ± 0.10	43.48 ± 0.08	42.64 ± 0.10	42.97 ± 0.10
1:8	40.31 ± 0.10	41.64 ± 0.08	41.94 ± 0.10	40.29 ± 0.10
1:7	40.62 ± 0.08	40.29 ± 0.07	42.98 ± 0.09	45.40 ± 0.10
1:6	39.82 ± 0.07	37.40 ± 0.01	42.98 ± 0.10	40.90 ± 0.09
1:5	31.02 ± 0.09	32.65 ± 0.10	38.76 ± 0.08	38.23 ± 0.09
1:4	32.01 ± 0.08	35.88 ± 0.06	46.97 ± 0.10	42.38 ± 0.09
1:3	31.14 ± 0.08	32.72 ± 0.08	35.71 ± 0.09	31.47 ± 0.08
1:2	31.42 ± 0.08	32.38 ± 0.10	34.93 ± 0.09	32.89 ± 0.09
1:1	33.98 ± 0.09	32.68 ± 0.09	34.95 ± 0.09	29.47 ± 0.08
1:0	28.26 ± 0.09	28.26 ± 0.09	27.93 ± 0.02	27.93 ± 0.02

The surface tension of pure water is measured at 72.02 mN/m, while they are 27.93 ± 0.02 mN/m for 0.15% APG solution and 28.26 ± 0.09 mN/m for 0.1% SDS solution. The surface tension of the composite solutions generally ranges from 31.15 ± 0.08 to 43.48 ± 0.08 mN/m. Compared with pure water, the surface tension of composite solutions significantly decreases. However, with the increasing proportion of the binding agent, the decreasing level becomes slighter until it eventually stabilizes. When the surfactant/binding agent ratio reaches 1:5, the surface tension of the composite solution drops below 40 mN/m. Based on the changes in surface tension values, a surfactant:binding agent ratio of 1:5 is relatively optimal.

2.3.2. Coal Powder Settling Velocity. The Walker test is an important method for studying solution wettability, characterizing the solution's ability to wet coal dust through settling tests.[24,25] Bituminous coal from Shenmu was selected as the test coal sample. The coal sample was sieved using a 200 mesh standard sieve to maintain coal dust particle sizes below 74 μm. Multiple 0.1 g coal dusts were weighed and uniformly sprinkled with a consistent force and angle, with the settling time being recorded each time. Shorter settling times indicate better wettability of the dust in the solution.

Experimental results show that for all surfactant and binding agent ratios, coal powder settling times exceed 10 min, mostly exhibiting slow descent until complete submersion is reached. This slow settling could be mainly attributed to the binding agent, which forms a liquid film on the surface of the composite solution, impeding rapid coal powder settling. When APG is combined with HMPC at a ratio of 1:5, the coal powder settling velocity in the composite solution is the fastest followed by the SDS and CMC-Na combination at a 1:5 ratio. Combining the surface tension study, the ratio of 1:5 is further confirmed.

2.3.3. Viscosity. Viscosity measurements were conducted using an NDJ-8S digital rotational viscometer. The prepared solutions were poured into containers. An appropriate rotor was selected and completely submerged in the solution for viscosity measurement. The viscosity of each solution was measured multiple times to obtain an average value, as shown in Figure 4.

The viscosity of pure water is typically around 1.23 mPa·s. The 0.15% APG solution has a viscosity of 1.37 mPa·s, while the 0.1% SDS solution has a viscosity of 1.18 mPa·s, close to that of water. In the composite mixed solutions, as the proportion of the wetting agent increases, the viscosity of the solution decreases with varying degrees. Overall, when the composite ratio is less than 1:2, the viscosity of the APG and HMPC combination solution is lower. At an APG:HMPC ratio
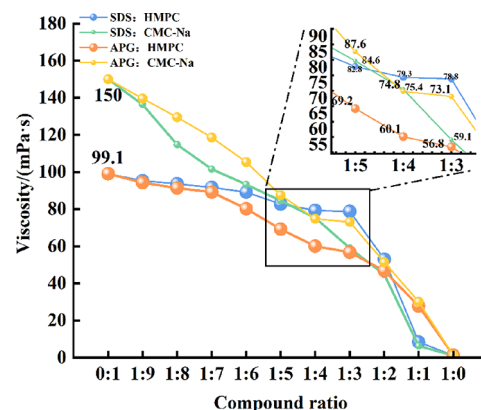

Figure 4. Change of viscosity of dust suppressants with different mixing proportions.

of 1:5, the viscosity of the solution is 69.2 mPa·s, while the viscosity values of other composite solutions are above 80 mPa·s. Moreover, when binding agents HMPC and CMC-Na are combined with surfactants APG and SDS, the viscosity at the same composite ratio is similar. For example, at APG:HMPC 1:3, the solution viscosity is 56.8 mPa·s. In contrast, for SDS:HMPC 1:3, the viscosity is 59.1 mPa·s. Similar viscosity values are observed for CMC-Na solutions at the same composite ratio. Viscosity values show little difference at composite ratios of 1:5, 1:4, and 1:3, and all composite solutions have viscosities below 40 mPa·s when the composite ratio exceeds 1:2. Combining the results of surface tension and settling velocity tests, the volume ratio of the surfactant to binding agent being 1:5 is deemed suitable.

3. ANALYSIS AND DISCUSSION OF THE DUST REDUCTION EFFECT

Infrared spectroscopy was adopted to analyze the change characteristics of functional groups of the coal before and after treatment of the composite dust suppressant, which could assist in the analysis of the dust suppression mechanism. Fourier transform infrared (FTIR) testing was performed using a Bruker solid–liquid two-phase infrared spectrometer. Shenmu bituminous coal with a 200 mesh was prepared and placed in water, SDS, APG, CMC-Na, HMPC, and each 1:5 composite solution to be immersed for 48 h. After soaking, the coal samples were dried in a vacuum drying oven for 24 h. The dried coal sample:KBr ratio was 1:99, which was pressed into the coal sheet.[26] Then, the coal sheet was put into the equipment for testing.

From Figure 5, it could be observed that the peak positions of coal samples treated with water, SDS, APG, CMC-Na,
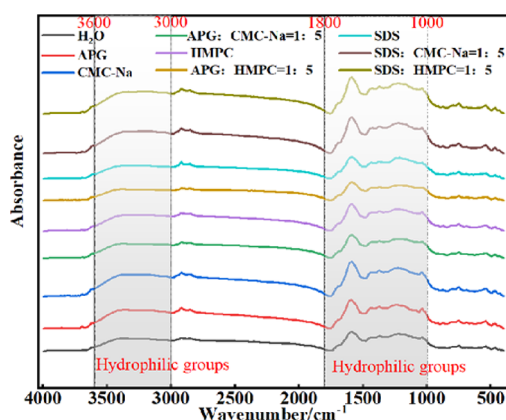

Figure 5. FTIR spectra of raw coal and treated coal.

HMPC, and the 1:5 composite solution are roughly the same. This indicates that the solution treatment does not cause a fundamental change in the structure of coal samples. However, the main content of each functional group changes. The absorption peak at 3600−3000 cm^{-1} is formed by hydroxyl stretching vibrations, while the absorption peaks in the range of 3000−2800 cm^{-1} correspond to the stretching vibrations of aliphatic hydrocarbons. The oxygen absorption peaks are concentrated in the range of 1800−1000 cm^{-1}, while the absorption peaks at 900−700 cm^{-1} correspond to the stretching vibrations of aromatic functional groups.[27] As

shown in Figure 5, the absorption peaks of oxygen-containing functional groups are more concentrated than those of the other functional groups.

Characteristic peaks in the FTIR spectrum can be fitted into four regions, as shown in Figure 6, with peak fitting data presented in Table 3. Hydroxyl- and oxygen-containing functional groups are classified as hydrophilic groups, while aliphatic and aromatic functional groups are considered hydrophobic groups. Compared to the original coal, the proportion of hydrophilic groups in the coal samples treated with CMC-Na solution increases the most, by 0.233%, while the proportion rises the least after treatment with HMPC solution, with only 0.052%. The coal samples treated with a composite solution of APG and CMC-Na show an increase of 0.088%. The coal samples treated with a composite solution of APG and HMPC show an increase of 0.004%, while those treated with SDS and CMC-Na have an increase of 0.095%, and those treated with SDS and HMPC show an increase of 0.144%. The proportion of hydrophilic groups in the coal samples treated with a composite solution of APG and HMPC is not as big as the corresponding SDS-treated one, indicating that the composite effect of SDS is better, leading to a bigger increase in the hydrophilic group area. Thus, selecting SDS for the composite is more reasonable. At the same time, it can be observed that after treatment with CMC-Na solution, the proportion of hydrophilic groups in the coal samples is the highest, reaching 97.51%. Similarly, the proportion of hydrophilic groups in the coal samples treated with SDS at a 1:5 ratio also reaches 97.37%, meeting the practical requirements of dust suppressants.
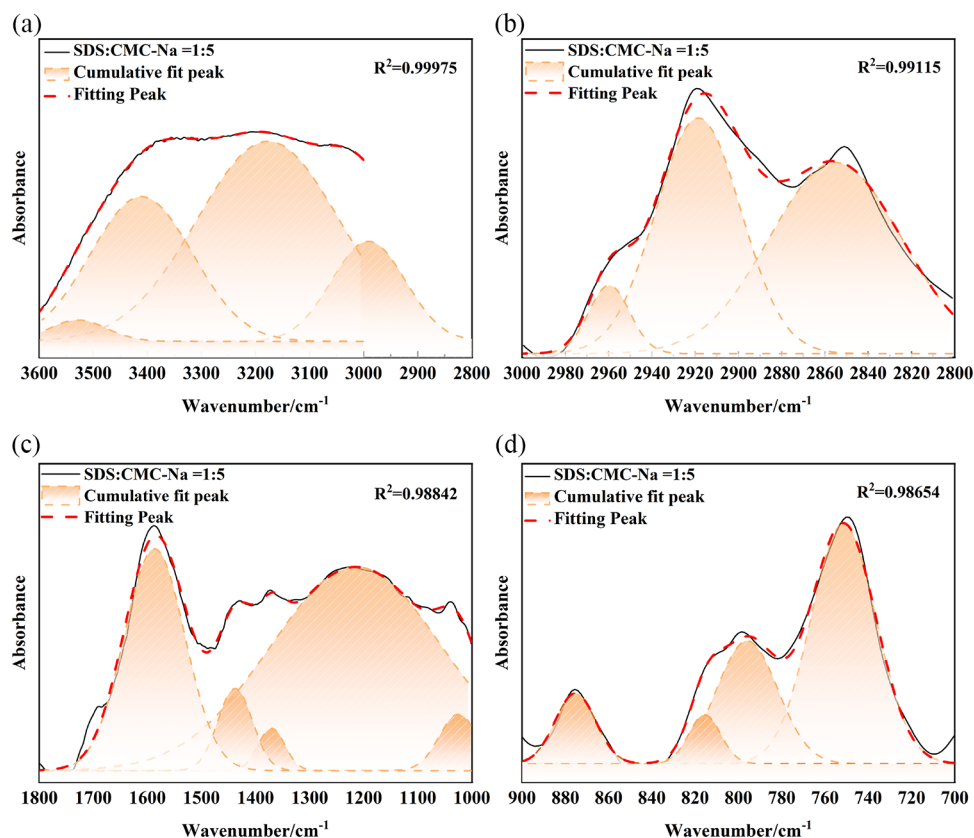

Figure 6. FTIR peak-differentiating fitting (SDS:CMC-Na = 1:5) at (a) wavenumber ranges of 3600−3000, (b) 3000−2800, (c) 1800−1000, and (d) 900−700.

Table 3. Peak-Differentiating Fitting of FTIR Data

wavenumber	H₂O (%)	APG (%)	SDS (%)	CMC-Na (%)	HMPC (%)	APG+CMC-Na (%)	APG+HMPC (%)	SDS+CMC-Na (%)	SDS+HMPC (%)
3600−3000	38.93	41.95	36.88	40.11	39.59	39.40	37.66	29.00	40.01
3000−2800	1.77	1.89	2.07	1.61	1.77	1.68	1.67	1.74	1.69
1800−1000	58.35	55.25	60.11	57.39	57.74	57.96	59.62	68.37	57.41
900−700	0.95	0.91	0.94	0.89	0.90	0.96	1.05	0.89	0.89
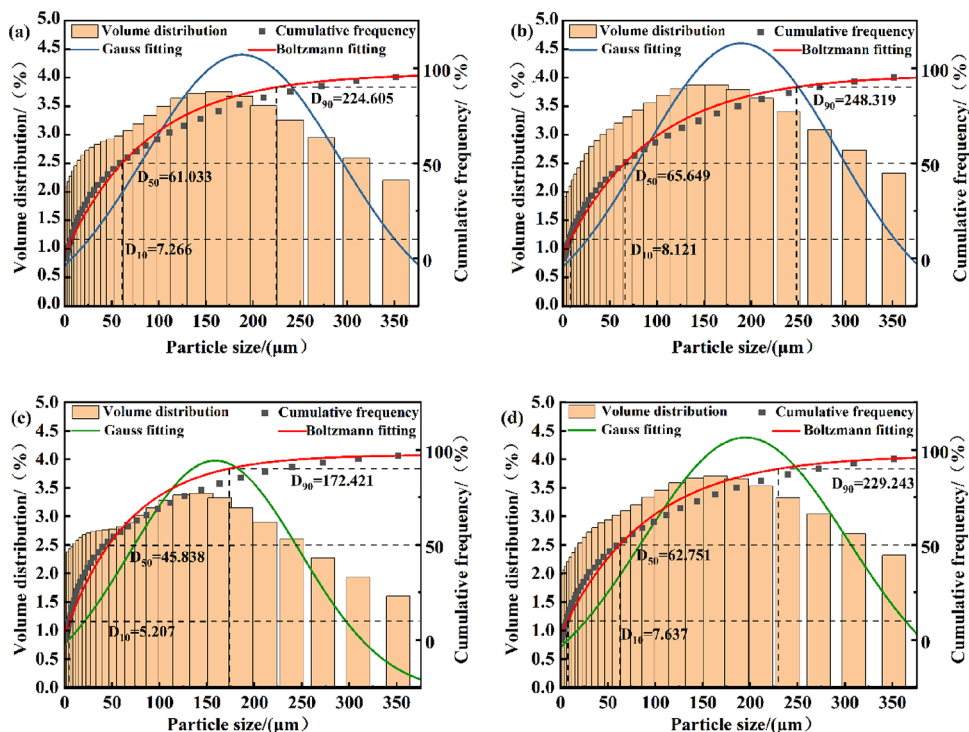
Figure 7. Particle size distribution of coal samples before and after treatment with a composite dust suppressant (a) before treatment of the Shenmu coal sample, (b) after treatment of the Shenmu coal sample, (c) before treatment of the Lucun coal sample, and (d) after treatment of the Lucun coal sample.

In order to investigate the dust suppression effect of composite dust suppressants (SDS:CMC-Na at a 1:5 ratio) on coal, a combination of gravity drop hammer tests and Malvern particle size experiments was conducted to analyze the changes in coal dust particle size before and after treatment with the dust suppressant.[28−30] Under negative pressure conditions, water and the composite dust suppressant solution were separately injected into coal samples. After soaking for 48 h, the samples were removed and dried in an oven at 50 °C for 24 h. Then, they were subjected to gravity drop hammer treatment and sieved through an 80-mesh sieve to obtain a coal powder. A laser diffraction particle size analyzer (Mastersizer 3000) was adopted to measure the particle size distribution of the coal powder. The particle size distribution pattern was studied based on the Boltzmann function model. The dust suppression performance was analyzed using characteristic particle size theory. The Boltzmann function is as follows.

$$y = A_2 + \frac{A_1 - A_2}{1 + e^{(\chi - \chi_0)/dx}} \qquad (2)$$

where χ is the particle size and y is the cumulative probability of particle size χ. A_1 and A_2 are parameters related to the characteristics of the distribution.

The characteristic particle size is the particle size corresponding to the cumulative particle size percentage of Dy*, i.e., the abscissa value corresponding to the intersection of the Boltzmann function distribution curve and $y = y^*$. The coal powder particle sizes obtained were fitted using the Boltzmann distribution function, as shown in Figure 7.[31] The dust suppression effects were evaluated based on the characteristic particle sizes (D_{10}, D_{50}, and D_{90}).[32]

There are differences in the particle size distribution of the two coal samples, but both are mainly below 75 μm, with most particles being below 200 mesh. The shapes of the particle size distributions of the two coal samples are similar, following a normal distribution pattern. The volume distribution peak of the original coal particles in both groups is lower than that of the treated coal. The volume distribution peak of Shenmu raw coal particles is concentrated in the range of 130−230 μm, while that of the treated Shenmu coal particles is in the range of 150−250 μm. The volume distribution peak of Lucun raw coal particles is in the range of 110−210 μm, The treated Lucun coal particles are concentrated in the range of 130−230 μm. Additionally, the volume distribution peak of the treated Lucun coal particles is above 200 μm, while for other coal samples, it is below 200 μm. The characteristic particle size reflects the particle size distribution of the coal powder after crushing. Compared with the original coal samples, the

characteristic particle sizes of the treated coal samples are larger. When the cumulative frequency is 50, the particle sizes after treatment with the composite dust suppressant are higher than those of the original coal samples. The particle size for Shenmu coal increases from 61.03 to 65.65 μm, and for Lucun coal, it increases from 45.84 to 62.75 μm. This indicates a corresponding reduction in dust generation capability after treatment with the composite dust suppressant solution, with the D_{10} characteristic particle size increasing by 11.77 and 46.67%, the D_{50} characteristic particle size increasing by 7.56 and 36.89%, and the D_{90} characteristic particle size rising by 10.56 and 32.96% for the two coal samples, respectively. These results demonstrate that the composite dust suppressant solution of CMC-Na and SDS can effectively weaken the dust generation capability of coal.

From the changes in functional groups, it could be observed that the proportion of hydrophilic groups in the coal samples treated with the SDS composite solution is higher than that treated with the APG composite solution. Moreover, the CMC-Na solution results in a higher proportion of hydrophilic groups compared with the HMPC solution, with more appropriate viscosity. Hence, the dust suppression effect of the composite dust suppressant solution of SDS and CMC-Na at a 1:5 ratio is good, which is also explained from the perspective of functional groups leading to the enlargement of the coal dust particle size distribution.

Furthermore, mechanical experiments were conducted to explain the reduced dust generation degree of coal by the composite dust suppressant from perspectives of coal cohesion and compressive strength.[33] Water and the composite dust suppressant solution were separately injected into coal samples under negative pressure conditions. The samples were soaked for 12, 24, and 48 h and then dried in an oven for 24 h. Uniaxial compression tests were carried out with a rock mechanics test system.[34−36] The force control mode was employed with a uniform loading rate of 1.00 kN/s until the specimens failed.[37]

The compressive strength R_i of the coal sample is calculated as

$$R_i = \frac{P}{A} \tag{3}$$

where R_i is the compressive strength of coal sample (MPa), P is the maximum load of coal sample damage (N), and A is the cross-sectional area of the coal sample (mm^2).

The shape correction factor is

$$K_{(h/d)} = \frac{8}{7 + 2\left(\frac{d}{h}\right)} \tag{4}$$

where $K_{(h/d)}$ is the Shape correction factor, d is the diameter of the coal sample (mm), and h is the height of the coal sample (mm).

The dimensional correction factor is

$$K_d = \left(\frac{50}{d}\right)^{0.18} \tag{5}$$

where K_d denotes the dimensional correction factor.

The standard uniaxial compressive strength of a single coal sample is

$$R = K_d K_{(h/d)} R_i = \left(\frac{50}{d}\right)^{0.18} \cdot \frac{8}{7 + 2\left(\frac{d}{h}\right)} \cdot \frac{P}{A} \tag{6}$$

Based on eq 6, the initial compressive strength σ_0 (original coal strength), the strength of water-treated coal samples σ_1, the strength of composite dust suppressant-treated (12 h) coal samples σ_{12}, the strength of composite dust suppressant-treated (24 h) coal samples σ_{24}, and the strength of composite dust suppressant-treated (48 h) coal samples σ_{48} are calculated. Their average value is obtained based on multiple experiments, as shown in Figure 8.
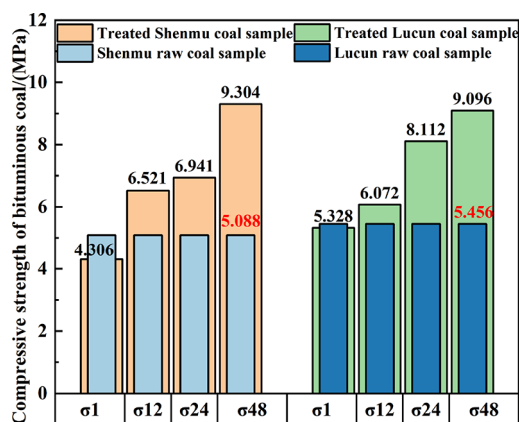

Figure 8. Compressive strength changes of coal samples.

It is evident that after treatment with composite dust suppressant solutions for different times, the compressive strength of both groups of coal increases compared to untreated coals, with a further growth in compressive strength with longer treatment times. In contrast, coal samples treated only with water show a slight decrease in compressive strength. After 48 h of treatment with the composite dust suppressant, the compressive strength of the Shenmu coal sample and the Lucun coal sample grow by 82.86 and 66.72%, respectively, compared to the original coal samples. Analysis of the fracture surface morphology of coal samples reveals a significant reduction in the degree of breakage at the coal surface after treatment with composite dust suppressant solution, which corresponds to the changes in compressive strength. Reasons could be explained as follows: the composite dust suppressant enters coal, combines with the coal particles, and forms a mesh structure inside the coal with good cohesion. This could act as a skeleton role for the coal as a whole, so as to obtain a higher strength. At the same time, the composite dust suppressant forms a cohesive substance on the inner surface of coal. Therefore, the composite dust suppressant could increase compressive strength of coal samples, lead to tighter bonding of coal particles internally, and reduce the degree of coal breakage. Good dust reduction effect is finally achieved.

4. CONCLUSIONS

Through experimental tests and theoretical model analyses, the characteristics of a new composite dust suppressant considering both bonding and wetting effects and its dust suppression mechanism are investigated. Conclusions are as follows:

1) The wettability of bituminous coal after treatment with a composite dust suppressant is superior to that treated with single binding agents, with the surface tension and

viscosity of dust suppressant solution decreasing by 54.8 and 43.6%, respectively. Variations in surface tension, viscosity, and coal powder settling time after dust suppressant treatment with 0.1% SDS solution and 0.4% CMC-Na solution (volume ratio of 1:5) are better. After composite dust suppressant treatment, the characteristic particle sizes (D_{10}, D_{50}, and D_{90}) of coal samples both become larger, with D_{10} increasing by 11.77 and 46.67%, D_{50} increasing by 7.56 and 36.89%, and D_{90} increasing by 10.56 and 32.96%, which reflects that the dust suppressant compounded with CMC-Na and SDS could effectively weaken the dust generation capacity of coal.

2) The proportion of hydrophilic groups in raw bituminous coal is 97.28%. This proportion in coal samples treated with APG and CMC-Na compounded solution rises by 0.088%, while coal samples treated with a composite solution of SDS and CMC-Na show an increase of 0.095%. The hydrophilic group percentage in coal samples treated with SDS compounded solution is higher than that treated with APG compounded solution. Meanwhile, the proportion of hydrophilic groups in coal samples treated with CMC-Na solution is the highest, which reaches 97.51%, which changes to be 97.37% in the case of SDS:CMC-Na being 1:5. The dust suppression effect is better, which is verified and analyzed from the perspective of functional groups.

3) After treatment with the composite dust suppressant for different times, the compressive strengths of both groups of bituminous coal increase. This increasing degree rises with a longer treatment time. However, coal samples treated with only water show a slight decrease in compressive strength. After 48 h of treatment, the compressive strengths of Shenmu and Lucun coal samples rise by 82.86 and 66.72%, respectively. The degree of breakage at the end face of coal largely reduces, which coincides with the change of compressive strength. Thus, a good dust reduction effect is realized. For future research, it is necessary to further study the dust suppression principle and the microstructure of the dust suppressant to obtain stronger synergistic effects. Meanwhile, more dust suppression field tests are expected.

AUTHOR INFORMATION

Corresponding Author

Chunshan Zheng − *Ministry of Education Key Laboratory of Safe and Effective Coal Mining and School of Safety Science and Engineering, Anhui University of Science and Technology, Huainan, Anhui 232001, China;* ◉ orcid.org/0000-0003-0255-6005; Email: chunshanzheng@aust.edu.cn

Authors

Suqian Qian − *Ministry of Education Key Laboratory of Safe and Effective Coal Mining and School of Safety Science and Engineering, Anhui University of Science and Technology, Huainan, Anhui 232001, China*

Bingyou Jiang − *Ministry of Education Key Laboratory of Safe and Effective Coal Mining and School of Safety Science and Engineering, Anhui University of Science and Technology, Huainan, Anhui 232001, China;* ◉ orcid.org/0000-0002-2751-7347

Sheng Xue − *Ministry of Education Key Laboratory of Safe and Effective Coal Mining and School of Safety Science and Engineering, Anhui University of Science and Technology, Huainan, Anhui 232001, China*

Xiaohan Wang − *Ministry of Education Key Laboratory of Safe and Effective Coal Mining and School of Safety Science and Engineering, Anhui University of Science and Technology, Huainan, Anhui 232001, China;* ◉ orcid.org/0000-0002-5670-6235

Cancan Li − *Ministry of Education Key Laboratory of Safe and Effective Coal Mining and School of Safety Science and Engineering, Anhui University of Science and Technology, Huainan, Anhui 232001, China*

Mingyun Tang − *Ministry of Education Key Laboratory of Safe and Effective Coal Mining and School of Safety Science and Engineering, Anhui University of Science and Technology, Huainan, Anhui 232001, China*

Complete contact information is available at:
https://pubs.acs.org/10.1021/acsomega.4c06012

Notes

The authors declare no competing financial interest.

REFERENCES

(1) Yan, J.; Wang, F.; Li, Y.; Gao, Y.; Li, Z.; Liu, H. A Feasibility Study of Coal Seam Water Injection Processes: The Effects of Coal Porosity and Mass Flow Rates of Injected Water on Wetting Radii. *Energy Fuels* **2020**, *34* (12), 16956−16967.

(2) Hu, Q.; Liu, S.; Li, Q.; Song, M.; Zhang, Y.; Sun, W.; Li, W.; Zhao, Z.; Zheng, X.; Wang, M.; Li, Z.; Song, J. Resistivity Response Characteristics of Coal and Coal-like Materials under Uniaxial Compression. *Energy Fuels* **2024**, *38* (10), 8598−8611.

(3) Xu, H.; Xu, J.; Zhai, C.; Yu, X.; Zheng, Y.; Sun, Y.; Zhu, X.; Chen, A. Quantitative Study of the Effects of Pore Structure and Wettability on the Water Spontaneous Imbibition Behaviors in Coal. *Energy Fuels* **2024**, *38* (1), 184−199.

(4) Ya, P.; Zhongan, J.; Shuo, F. E. H.; Gui, L. Research on optimization and effect of water injection and dust prevention in coal seam in fully mechanized mining working face. *Coal Sci. Technol.* **2018**, *46* (01), 224−230.

(5) Xiaotao, Z. Research on the application of water injection and dust reduction technology in fully mechanized coal seam mining working faces with high gas outbursts. *Coal Sci. Technol.* **2019**, *47* (01), 231−236.

(6) Yansong, Z. Research on the mechanism of using wetting agents to improve coal seam water injection effect. *Mech. Eng.* **1995**, No. 03, 54−57.

(7) Chao, W. Basic research on chemical dust suppressants and their application in mines. *Min. Bull. Min. Express* **2001**, No. 12, 5−7 + 15.

(8) Chao, W.; Zhixing, Z.; Jiacai, O.; Bo, Z.; Zijun, L. Correlation between different experimental devices for measuring the wetting effect of dust wetting agents. *Chin. J. Nonferrous Met.* **2005**, *10*, 136−141.

(9) Yunhang, W.; Shuguang, J.; Guangmin, C.; Zhengyan, W.; Lianghai, L. Experimental study on improving coal seam water injection effect by compound wetting agent. *Saf. Coal Mines* **2014**, *45* (07), 9−11 + 15.

(10) Haifei, L.; Baoli, L.; Min, Y.; Yang, B. Research on the effect of non-cationic surfactants on coal wetting properties. *China Saf. Sci. J.* **2018**, *28* (05), 123−128.

(11) Zongqi, H.; Shaocheng, G.; Liying, S.; Xiaowei, Z.; Xi, C. Research on compounding of high-efficiency bituminous coal dust suppressant. *China Coal* **2022**, *48* (03), 62−67.

(12) Chao, Z.; Xinglong, W.; Shugang, L.; Bingyou, J.; Cheng, Z.; Chuanjie, Z.; Guanhua, N. Development and application of a new compound wetting agent for coal seam water infusion. *Fuel* **2022**, *314*, No. 122767.

(13) Zhang, W.; Hu, Q.; Jiang, S.; Wang, L.; Chai, J.; Mei, J. Experimental study on coal dust wettability strengthened by surface active ionic liquids. *Environ. Sci. Pollut. Res.* **2022**, *29* (30), 46325−46340.

(14) Xie, J.; Xie, J.; Jiang, B.; Sun, Q. Experimental Research on the Performance of a Wetting Agent Based on Compound Acidification in Low-Porosity and Hard-to-Wet Coal Seams. *ACS Omega* **2021**, *6* (40), 26680−26688.

(15) Xu, L.; Li, Y.; Du, L.; Yang, F.; Zhang, R.; Wei, H.; Wang, G.; Hao, Z. Study on the effect of SDBS and SDS on deep coal seam water injection. *Sci. Total Environ.* **2023**, *856* (P2), No. 158930.

(16) Liu, Z.; Zhu, M.; Yang, H.; Zhao, D.; Zhang, K. Study on the influence of new compound reagents on the functional groups and wettability of coal. *Fuel* **2021**, *302*, No. 121113.

(17) Liang, Z. *Study on the relationship between microstructure and properties of hydroxypropyl methylcellulose/hydroxypropyl starch blend system*; [D]. South China University of Technology: 2015.

(18) Xi, Z.; Wang, C.; Xia, T.; Suo, L. Synthesis of a new three-dimensional cross-linked network dust suppressant and its mechanism of coal-dust inhibition. *Powder Technol.* **2023**, *430*, No. 118976.

(19) Jiahao, L.; Jun, C.; Chengfei, L.; Jianxiao, Y. Effect of asphalt binder on the preparation and performance of low-rank coal-based activated coke. *Coal Process. Compr. Util.* **2022**, No. 07, 65−75.

(20) Rahmati, K.; Saradar, A.; Mohtasham Moein, M.; Sardrinejad, I.; Bristow, J.; Yavari, A.; Karakouzian, M. Evaluation of Engineered Cementitious Composites (ECC) containing Polyvinyl Alcohol (PVA) fibers under compressive, direct tensile, and drop-weight test. *Multiscale and Multidiscip. Model. Exp. and Des.* **2022**, *6* (1), 147−164.

(21) Jian, D.; Di, W. Experimental and application research on coal seam water injection and dust prevention based on wetting agent addition. *Coal Mine Mach.* **2022**, *43* (12), 149−152.

(22) Jingbo, F. Experimental study on adding surfactant to improve coal seam water injection effect. *Shandong Coal Sci. Technol.* **2021**, *39* (10), 90−92 + 128.

(23) Xiaohua, G.; Wei, C.; Shangquan, M.; Maozeng, Z. Application experiment of surfactants in dust prevention in coal mines. *Min. Saf. Environ. Prot.* **2010**, *37* (03), 27−30.

(24) Gang, Z.; Weimin, C.; Gang, W.; Wen, N. Surfactant dust removal technology for fully mechanized caving working surface. *Ind. Saf. Environ. Prot.* **2009**, *35* (11), 17−19.

(25) B, A. R.; G, A. S.; S, A. A. Evaluation of the effectiveness of wetting coal particles with various reagents to reduce air dustiness. *Bulletin of the Kuzbass State Technical University* **2021**, *148* (6).

(26) Ma, Y.; Sun, J.; Ding, J.; Liu, Z. Synthesis and characterization of a penetrating and pre-wetting agent for coal seam water injection. *Powder Technol.* **2021**, *380*, 368−376.

(27) Wang, X. H.; Jiang, B.; Yuan, L.; Zhao, Y.; Yu, C. F.; Zheng, Y.; Huang, J.; Ji, B. Study on coupling chelating agent and surfactant to enhance coal wettability: Experimental and theoretical discussion. *Fuel* **2023**, *342*, No. 127861.

(28) Zhang, C.; Ren, Z.; Hao, D.; Zhang, T. Numerical Simulation of Particle Size Influence on the Breakage Mechanism of Broken Coal. *Arabian J. Sci. Eng.* **2020**, *45* (11), 9171−9185.

(29) Zhang, Z. Particle overlapping error correction for coal size distribution estimation by image analysis. *Int. J. Miner. Process.* **2016**, *155*, 136−139.

(30) Huaiguang, G. Experimental study on the strength of gas-containing coal and rock mass based on the falling weight method. *Saf. Coal Mines* **2019**, *50* (08), 10−13.

(31) Song, S.; Pang, M.; Guo, Y.; Zhang, L.; Zhang, T.; Pan, H. Experimental Investigation of the Non-Darcy Equivalent Permeability of Fractured Coal Bodies: The Role of Particle Size Distribution. *Fractal Fractional* **2023**, *7* (6), 423.

(32) Hou, J.; Hu, X.; Zhao, Y.; Shao, Z.; Cheng, W.; Zhu, S.; Song, C.; Zhu, F. Improvement of wettability of coal seams in water injection via co-deposition of polydopamine and polyacrylamide. *Colloids Surf., A* **2022**, *636*, No. 128112.

(33) Yanhe, L.; Cheng, Z.; Aikun, C.; Hong, Z. Research on uniaxial loading failure characteristics of coal-rock combinations with different strengths. *Coal Eng.* **2023**, *55* (06), 108−112.

(34) Boutrid, A.; Chettibi, M.; Yahyaoui, S.; Talhi, K. Investigations of strength properties of sandstone rock. *World J. Eng.* **2015**, *12* (1), 13−18.

(35) Yang, E.; Li, S.; Lin, H.; Zhao, P.; Qin, L.; Zhao, B. Influence mechanism of coal thickness effect on strength and failure mode of coal−rock combination under uniaxial compression. *Environ. Earth Sci.* **2022**, *81* (17), 429.

(36) Yang, K.; Wei, Z.; Chi, X.; Zhang, Y.; Dou, L.; Liu, W. Experimental Research on the Mechanical Characteristics and the Failure Mechanism of Coal-Rock Composite under Uniaxial Load. *Adv. Civ. Eng.* **2020**, *2020*, 8867809.

(37) Zhang, P.; Wang, J.; Jiang, L.; Zhou, T.; Yan, X.; Yuan, L.; Chen, W. Influence Analysis and Stepwise Regression of Coal Mechanical Parameters on Uniaxial Compressive Strength Based on Orthogonal Testing Method. *Energies* **2020**, *13* (14), 3640.